Original Article
Running Title: α -Tocopherol and Cetuximab Treatment
Received: June 26, 2026; Accepted: November 2, 2026

α -tocopherol Suppresses Epithelial–Mesenchymal Transition Associated Cellular and Cytoskeletal Regulators Mechanisms during Cetuximab Treatment in Breast Cancer

Mehmet Aytar[*], PhD, Demet Yalcin[*], PhD, Ozge Cevik[**♦], PhD

[*]*ADU-Science and Technology Application and Research Center, Aydin Adnan Menderes University, Aydin, Turkey*
[**]*Department of Medicinal Biochemistry, School of Medicine, Aydin Adnan Menderes University, Aydin, Turkey*

♦Corresponding Author
Ozge Cevik, PhD
Department of Medicinal Biochemistry,
School of Medicine,
Aydin Adnan Menderes University,
Aydin, Turkey
Email: ozge.cevik@adu.edu.tr

Abstract

Background: The cellular interactions between cetuximab and antioxidant compounds such as α-tocopherol remain unclear. The present study investigated the effects of their combined treatment on epithelial–mesenchymal transition (EMT) associated cytoskeletal regulators in breast cancer cells.

Method: In this in-vitro experimental study, MCF-7 cells were treated with cetuximab and/or α-tocopherol, and the effects of the treatments were evaluated at 72 h and 7 days. Cell proliferation and colony-forming potential were assessed, and the levels of Vav-1, Rac-1, and F-actin proteins were determined. Actin-associated protein distribution was further evaluated by SDS-PAGE analysis of ultracentrifugation-derived F-actin- and G-actin-enriched cellular fractions. Statistical comparisons were performed using ANOVA.

Results: Combined treatment with cetuximab (250 µg/mL) and α-tocopherol (50 µM) significantly inhibited cell proliferation at 24, 48, and 72 h and suppressed colony formation after 7 days compared with the control and single-treatment groups. The combined treatment also significantly reduced Vav-1 and Rac-1 protein levels and altered F-actin organization. Furthermore, the combination treatment was associated with reduced actin-associated protein signals in the F-actin-enriched fraction and suppressed the acquisition of a mesenchymal-like phenotype in MCF-7 cells.

Conclusion: Beyond its antioxidant capacity, α-tocopherol modulates intracellular signaling pathways involved in cancer inhibition. Despite its therapeutic potential, its dietary administration in oncology remains controversial. The combined treatment with cetuximab and α-tocopherol

altered EMT signaling and cytoskeletal dynamics in MCF-7 cells, suggesting a potential role in modulating cellular processes associated with cancer progression.

Keywords: alpha-tocopherol, Cetuximab, MCF-7, Breast neoplasms, Epithelial-mesenchymal transition

Introduction

Breast cancer is the most commonly diagnosed cancer among women worldwide and the second most commonly diagnosed cancer globally, representing a major public health burden due to its substantial morbidity and mortality. Therefore, various treatment methods have been developed over time, including hormonal therapy, chemotherapy, targeted therapies, and immunotherapy. However, the heterogeneous nature of breast cancer makes effective treatment challenging. [1, 2] Breast cancer is classified based on the presence of receptors such as progesterone and estrogen hormone receptors, and human epidermal growth factor receptor 2 (HER2), which are often found in overexpressed on the membranes of cancer cells. Breast cancers are commonly classified according to the expression of estrogen receptor (ER), progesterone receptor (PR), and HER2. Tumors expressing ER, PR, or HER2 are described as hormone receptor-positive or HER2-positive breast cancer, respectively. Tumors that co-express ER, PR, and HER2 are referred to as ER/PR/HER2-positive or triple-positive breast cancer. These receptor profiles provide important information about tumor biology and help guide treatment selection. Clinical classifications provide information about tumor characteristics, guiding the selection of the most appropriate treatment. For example, in ER/PR positive tumors, endocrine therapies such as tamoxifen or aromatase inhibitors are preferred to reduce the risk of recurrence after surgery. In tumors with HER2 overexpression, monoclonal antibody therapy called Herceptin (Trastuzumab), which suppresses cell proliferation by binding to the receptor, is applied. HER2 and epidermal growth factor receptor (EGFR) are members of the ErbB receptor tyrosine kinase family and can interact through receptor heterodimerization and functional cross-talk. In breast cancer, EGFR–HER2 heterodimers have been implicated in oncogenic signaling and may contribute to tumor cell proliferation, motility, and metastatic progression.[3] Aberrant EGFR signaling has also been associated with epithelial-mesenchymal transition (EMT) related cellular changes, suggesting that interactions between ErbB family receptors may influence epithelial and mesenchymal phenotypes in breast cancer.[4, 5] Therefore, targeting EGFR signaling may represent a potential complementary strategy in selected breast cancer settings. Cetuximab is the first chimeric monoclonal antibody to specifically bind to the extracellular region of EGFR, and is an FDA-approved therapeutic agent.[6] However, the clinical efficacy of EGFR inhibitors is limited; this necessitates a better understanding of resistance and EMT mechanisms.[7] EMT is a process involving a dynamic transition between epithelial and mesenchymal phenotypes, where cells lose their epithelial characteristics and acquire more motile and invasive mesenchymal characteristics due to changes in their cytoskeleton and adhesion molecules.[8, 9] Findings from studies investigating the role of cytokines in the EMT process in breast cancer show that cytokines such as transforming growth factor-beta (TGF-β), interleukin-6 (IL-6), and tumor necrosis factor-alpha (TNF-α) trigger EMT,

decreasing epithelial markers such as E-cadherin and β-catenin, while increasing mesenchymal markers such as vimentin, N-cadherin, and fibronectin. Furthermore, transcription factors such as Snail, Twist, and ZEB are activated. These changes increase cell motility, invasion, and metastasis, while also contributing to treatment resistance. Therefore, cytokines and EMT associated regulators are considered potential targets in breast cancer treatment.[10] In addition to these canonical EMT markers, alterations in intracellular signaling and cytoskeletal organization are important components of the EMT-associated phenotype. Vav-1 and Rac-1 are involved in signaling pathways that regulate actin cytoskeletal dynamics,[11] cell shape, and cellular motility, while F-actin constitutes a major structural component of the cytoskeleton.[12] Therefore, changes in Vav-1, Rac-1, and F-actin may provide complementary information regarding cellular and cytoskeletal responses associated with EMT. In the present study, these molecules were selected to investigate EMT-associated cytoskeletal and signaling processes. Therefore, Vav-1, Rac1, and F-actin were investigated the effects of cetuximab and α-tocopherol on EMT-associated signaling and cytoskeletal components rather than as replacements for canonical EMT markers.

Although cetuximab is not an established standard treatment for breast cancer, EGFR-targeted combination strategies have been investigated in advanced and metastatic breast cancer, including metastatic triple-negative breast cancer, where the addition of cetuximab to cisplatin showed an improvement in progression-free survival compared with cisplatin alone. Cetuximab has been investigated in relation to EMT in several cancer models. In patients with head and neck squamous cell carcinoma, cetuximab treatment was associated with changes in genes and signaling pathways related to EMT and cancer-associated fibroblasts, suggesting that EMT-related processes may contribute to the biological response to anti-EGFR therapy. Similarly, in feline oral squamous cell carcinoma cells, cetuximab was reported to modulate EMT-associated processes, matrix metalloproteinase activity, and cell migration in-vitro.[13] These findings indicate that the effects of cetuximab on EMT-related cellular processes may vary according to tumor type and cellular context. However, the effects of cetuximab in combination with bioactive compounds such as α-tocopherol on EMT-associated cytoskeletal regulation in breast cancer cells remain poorly characterized. Therefore, rather than focusing exclusively on canonical EMT markers, the present study investigated complementary EMT-associated cellular and cytoskeletal processes, including Vav-1 and Rac-1 expression and F-actin organization and polymerization, in MCF-7 breast cancer cells.

Tocopherols are common fat-soluble antioxidants found in vegetable oils.[14, 15] Of the eight forms of vitamin E, α-tocopherol is the most common and biologically active.[16, 17] α-tocopherol provides protection against reactive oxidative stress (ROS) induced lipid peroxidation through its antioxidant effect.[18, 19] This strong antioxidant effect stems from the phenolic structure and electron-donating groups in the aromatic ring. ROS are reactive molecules formed by electron transfer from oxygen and have an impact on chronic diseases, food spoilage, and environmental systems.[20, 21] Developing protective strategies against these processes is critical for health and food production. α-tocopherol acts not only as an antioxidant but also as a modulator of intracellular signaling, suggesting its potential role in inhibiting cancer cell progression. Whether it should be included in or excluded from the diets of

cancer patients remains a subject of ongoing debate. Accordingly, the present study aimed to investigate the effects of cetuximab and α-tocopherol, alone and in combination, on MCF-7 breast cancer cells, with particular emphasis on cell proliferation, colony-forming capacity, and the EMT-associated signaling and cytoskeletal components Vav-1, Rac-1, and F-actin.

Materials and Methods

Cell culture and cell proliferation assay

This in-vitro experimental study used a human breast cancer MCF-7 cell line (ATCC® HTB-22™) obtained directly from the American Type Culture Collection (ATCC, Manassas, VA, USA). The cells were used at passage 14. The cells were maintained under culture conditions as DMEM medium containing 10% fetal bovine serum (FBS), 2 mM L-glutamine, 100 U/mL penicillin, and 100 µg/mL streptomycin. Cells were maintained in an incubator at 37 °C in a humidified atmosphere containing 5% CO_2.

Cetuximab (Erbitux®; Merck Healthcare KGaA, Darmstadt, Germany) was diluted with sterile 0.9% sodium chloride solution to obtain the desired working concentrations. α-Tocopherol (catalog no. 258024; Sigma-Aldrich) was dissolved in dimethyl sulfoxide (DMSO) and subsequently diluted to the required concentrations. For the vehicle control group, sterile 0.9% sodium chloride solution and DMSO were added to the culture medium at concentrations equivalent to those used in the treatment groups, with the final DMSO concentration maintained below 1%. This vehicle control was used to account for any potential effects of the solvents on MCF-7 cell responses.

The required sample size was determined using the online sample size and power calculation tool (https://powerandsamplesize.com) based on an a priori power analysis. The analysis indicated that a minimum of three independent experiments was required to detect statistically significant differences between the experimental groups. All experiments were independently repeated three times (n = 3 biological replicates). For each independent experiment, each treatment condition was analyzed in duplicate technical replicates, and the mean value of the technical replicates was used for statistical analysis.

To determine cell viability, attachment cells were treated with trypsin-EDTA and seeded in 96-well plates (1×10^4 cells/well). Cells were treated with different concentrations of Cetuximab (Cet, 50-100-250-500 µg/mL) and/or α-Tocopherol (αToc, 10-50-100 µM) and incubated for 24, 48, and 72 hours. Following incubation, 10 µL of MTT labeling reagent was added to each well, and the cells were incubated for 4 hours at 37 °C in a humidified atmosphere containing 5% CO_2. After incubation, 100 µL of DMSO was added to each well to dissolve the formed formazan precipitates. Finally, absorbance measurements were performed using a microplate reader at a wavelength of 570 nm, and each experiment was conducted in triple replicates.[22]

Vav-1, Rac-1, and F-actin protein measurement

MCF-7 cells were seeded into 12-well plates at a concentration of 5×10^4 cells per well in 800 µL of medium.[23] Bright-field microscopy images were taken after 24, 48, and 72 hours with inverted microscope (Zeiss Axio Vert.A1, Germany). After cell adherence to the surface, Cet (250 µg/mL) and/or αToc (50 µM) were added and incubated for 72 hours and 7 days. The cells were collected and lysed with RIPA lysis buffer (Millipore, 20-188) The protein concentrations were measured using BCA kits (SMART™ BCA Protein Assay Kit,

Intron Biotechnology 21071). Vav-1, Rac-1, and F-actin levels were determined using commercially available ELISA kits for Vav-1 (SunRed Biotechnology, Cat. No. 201-12-5233), Rac-1 (SunRed Biotechnology, Cat. No. 201-12-6937), and F-actin (SunRed Biotechnology, Cat. No. 201-12-7313), respectively, according to the manufacturer's instructions. The analytical characteristics of the ELISA kits were obtained from the manufacturer's specifications. The assay sensitivity was 0.428 ng/mL for F-actin, 0.049 ng/mL for Rac-1, and 11.869 ng/mL for Vav-1, with corresponding assay ranges of 0.5–100 ng/mL, 0.05–15 ng/mL, and 12.5–3200 ng/mL, respectively. The intra-assay coefficient of variation (CV) was <10%, and the inter-assay CV was <12%. To account for differences in total protein content among samples, the measured concentrations of Vav-1, Rac-1, and F-actin protein were normalized to the corresponding total protein concentration of each sample. The normalized values were used for subsequent statistical analyses.

Actin-associated protein distribution analyses

MCF-7 cells were seeded into 12-well plates. They were then treated with Cet (250 µg/mL) and/or αToc (50 µM) and incubated at 37 °C for 72 hours. After incubation, the wells were washed with phosphate buffered saline (PBS). For cellular fractionation, cells were lysed using commercially RIPA lysis buffer (Millipore, 20-188) supplemented with protease inhibitor cocktail (Sigma-Aldrich, P8340). Briefly, 200 µL of ice-cold RIPA lysis buffer containing protease inhibitor cocktail was added to each well, and the cells were incubated on ice for 15 min. The cells were then mechanically disrupted, and the lysates were transferred to ultracentrifuge tubes. Equal volumes of the samples were subjected to ultracentrifugation at 100.000 × g for 1 h at 4°C using an Optima MAX-XP ultracentrifuge (Beckman Coulter). Following centrifugation, F-actin-enriched pellet fraction and G-actin-enriched supernatant fraction were carefully separated. The pellet was resuspended in an equal volume of RIPA lysis buffer supplemented with protease inhibitor cocktail. F-actin/G-actin enriched fractions were evaluated by SDS-PAGE.[24] A resolving SDS-PAGE gel with a resolving power of 14% was prepared and run at 120 volts for a duration of one hour. The samples were loaded at a concentration of 30 µg per well. A volume of 5 µL marker (GangNam-STAIN Prestained Protein Ladder, Intron Biotechnology 24052) was used. Quantification analyses were then compared using a gel imaging system (Syngene GBOX image system).

Colony formation assay

MCF-7 cells were seeded into 12-well plates at a concentration of 1000 cells per well. They were then treated with Cet (250 µg/mL) and/or αToc (50 µM) and incubated at 37°C for 7 days. The culture medium was changed every 3 days. At the end of the incubation period, each well in the plate was washed with PBS. The cells were then fixed with cold methanol/acetic acid, stained with 0.5% crystal violet staining solution for 15 minutes, and washed with double distilled water (ddH_2O). The stained cells were examined and visualized under a microscope. The number of colonies in each well was counted and analyzed with microscope (Zeiss Axio Vert.A1, Germany).[22]

Statistical analysis

The statistical analysis of the data was conducted using GraphPad Prism 7.0 (GraphPad Software, USA). Quantitative data are expressed as mean ± standard deviation (SD). The Kolmogorov-Smirnov and Shapiro-Wilk tests were used to ascertain the normal distribution of the obtained data. The analysis performed was a one-way analysis of variance (ANOVA) test, which

was used to facilitate the undertaking of multiple comparisons (Tukey's HSD). Statistically significant results were considered to be those with *P*-values of 0.05 or less.

Results

Cell proliferation was evaluated at 24-, 48-, and 72-hours following treatment with cetuximab and/or α-tocopherol in MCF-7 cells. When the same number of cells was seeded, a progressive increase in cell number was observed in the control group at all time points (24, 48, and 72 hours, Figure 1a). No significant changes were observed in the Cet and/or αToc groups compared with the control group after 24 hours of incubation. After 48 and 72 hours of incubation, a significant decrease was observed in each group in the Cet and/or αToc groups compared with the control group ($P < 0.001$). In the groups where combinations were used, comparisons were made between the amounts of Cet and αToc added to the cells and the amounts added individually over the same time period. Accordingly, in the Cet (100 µg/mL) + αToc (10 µM) group, cell proliferation decreased significantly after 48 hours of incubation compared with the αToc (10 µM) group alone, but this change was not observed after 72 hours ($P < 0.05$). In the Cet (250 µg/mL) + αToc (50 µM) group, cell proliferation was significantly reduced after 48 hours of incubation compared with the αToc (50 µM) group alone ($P < 0.05$) and the Cet (250 µg/mL) group alone ($P < 0.05$). After 72 hours of incubation, cell proliferation was also reduced in the Cet (250 µg/mL) + αToc (50 µM) group compared with the αToc (50 µM) group alone ($P < 0.05$) and the Cet (250 µg/mL) group alone ($P < 0.01$). Morphological evaluation revealed that cells in the control group tended to aggregate and maintained their typical epithelial morphology after 72 hours (Figure 1b). Treatment with Cet (250 µg/mL) and αToc (50 µM) resulted in visible changes in cell morphology and cellular organization, including increased cell rounding and irregular cell shapes compared with the corresponding untreated controls.

Colony formation capacity was evaluated in MCF-7 cells following treatment with Cet (250 µg/mL) and/or αToc (50 µM) for 7 days. After the incubation period, prominent colony formation was observed in the control group, whereas colony formation was markedly suppressed in cells treated with Cet alone and in the combination treatment with Cet and αToc. Morphological evaluation revealed that cellular clustering and colony expansion were significantly reduced in the treated groups (Figure 2a). In particular, reduced cellular protrusions and decreased cell–cell interactions suggested that EGFR inhibition by Cet disrupted cellular communication and colony expansion. Quantitative analysis (Figure 2b) based on colony counting demonstrated a significant reduction in colony numbers in all treatment groups compared with the control group (Cet, $P < 0.001$; αToc, $P < 0.001$; Cet+αToc, $P < 0.001$). Notably, the combination of Cet and αToc resulted in a significantly greater suppression of colony formation compared with Cet ($P < 0.01$) and αToc ($P < 0.01$), indicating an enhanced inhibitory effect on the clonogenic potential of MCF-7 cells.

The levels of Vav-1, Rac-1, and F-actin protein, key markers involved in EMT signaling, were evaluated in both cell secretions (supernatant) and cell pellets of MCF-7 cells following treatment with cetuximab (250 µg/mL) and/or α-tocopherol (50 µM) at 72 hours and 7 days (Figure 3).

At 72 hours, Vav-1 protein levels in the cell-derived supernatant were increased in the Cet group, whereas the Cet + αToc group showed lower Vav-1 levels compared with cetuximab alone (Figure 3a). No significant differences

were detected among groups in the 72-hours cell pellets. At 7 days, Vav-1 levels in the cell-derived supernatant were significantly reduced in both the αToc ($P < 0.01$) and Cet + αToc ($P < 0.01$) groups compared with the corresponding control group. In the 7-day cell pellets, Vav-1 protein levels were significantly increased in the Cet group compared with the control group ($P < 0.001$), whereas the Cet + αToc group showed a significant reduction compared with the Cet group ($P < 0.01$). No significant changes were observed in Vav-1 levels in the αToc group in either the supernatant or pellet fractions. Overall, these findings demonstrate time- and fraction-dependent changes in Vav-1 protein levels following treatment.

Rac-1 protein levels in the 72-hours cell-derived supernatant were significantly decreased in both the αToc ($P < 0.05$) and Cet + αToc ($P < 0.05$) groups compared with the corresponding control group, whereas no significant changes were observed in the 72-hours cell pellets (Figure 3b). At 7 days, Rac-1 protein levels in the cell-derived supernatant were significantly reduced in the Cet + αToc group compared with both the control ($P < 0.05$) and Cet ($P < 0.05$) groups. In the 7-day cell pellets, Rac-1 protein levels were significantly decreased in the Cet ($P < 0.01$), αToc ($P < 0.01$), and Cet + αToc ($P < 0.001$) groups compared with the corresponding control group. Furthermore, Rac-1 protein levels in the Cet + αToc group were significantly lower than those in the Cet group ($P < 0.01$). Overall, these findings demonstrate differential, time- and fraction-dependent changes in Rac-1 protein levels following treatment, with changes observed in both cell-derived supernatant and cell-associated fractions.

For F-actin protein levels, no significant differences were observed among the treatment groups at 72 hours in either the cell-derived supernatant or cell pellet fractions (Figure 3c). At 7 days, F-actin protein levels in the cell-derived supernatant were significantly reduced in the αToc ($P < 0.05$) and Cet + αToc ($P < 0.01$) groups compared with the corresponding control group. In addition, F-actin protein levels were significantly lower in the Cet + αToc group than in the αToc group ($P < 0.05$). Similarly, in the 7-days cell pellet fractions, F-actin levels were significantly decreased in the Cet + αToc group compared with the control ($P < 0.05$), αToc ($P < 0.05$), and Cet ($P < 0.05$) groups. F-actin- and G-actin-enriched fractions were further evaluated by SDS-PAGE following ultracentrifugation (Figure 3d). The F-actin-enriched pellet fraction showed qualitatively weaker actin-associated bands in the Cet + αToc group compared with the control and single-treatment groups. A similar reduction in band intensity was observed in the corresponding G-actin-enriched supernatant fraction. These findings suggest treatment-associated alterations in the distribution of actin between the F-actin- and G-actin-enriched fractions.

Discussion

In the present study, combined treatment with cetuximab and α-tocopherol produced a greater inhibitory effect on MCF-7 cell proliferation and colony formation than either treatment alone and was associated with time- and fraction-dependent alterations in Vav-1, Rac-1, and F-actin, indicating modulation of cellular and cytoskeletal processes associated with EMT. These findings provide preliminary evidence that α-tocopherol may modify the cellular response to cetuximab through changes in cytoskeletal organization and EMT-associated signaling, although the present data do not establish direct inhibition of EMT or specific resistance mechanisms.

EGFR is generally expressed higher levels in tumor cells than in normal cells. Because of

this overexpression, EGFR represents an important target for cancer therapy.[25] EGFR plays a critical role in the regulation of growth, proliferation, survival, and differentiation processes in mammalian cells.[26]

When cetuximab blocks the EGFR receptor and interrupts growth signaling, cancer cells tend to activate alternative pathways to overcome this blockade and maintain survival. The concentrations of cetuximab used in the present study should be considered within the context of an in-vitro experimental model rather than direct equivalents of clinical exposure. The 250–500 µg/mL concentrations of cetuximab are higher than the average circulating concentrations reported in patients receiving standard cetuximab treatment. However, relatively high concentrations of cetuximab have been used in previous in-vitro studies, particularly in MCF-7 cells, which have been reported to exhibit relatively low sensitivity to cetuximab, with an IC50 not reached even at concentrations up to 100 µg/mL. Therefore, the higher concentrations used in the present study were selected to obtain a measurable pharmacological response in the MCF-7 model, and to evaluate the potential modulatory effect of α-tocopherol under conditions of cetuximab exposure. Although cetuximab is not an established standard treatment for breast cancer, EGFR-targeted therapeutic strategies have been investigated in combination with other agents in selected breast cancer settings. However, the potential interactions between EGFR-targeted therapies and bioactive compounds commonly used as nutritional supplements, such as α-tocopherol, remain insufficiently characterized. In many cases, tumor cells upregulate other receptor tyrosine kinases such as Axl, MET, or HER3. These receptors activate Rac-1, a cytoskeletal regulator, enabling cancer cells to maintain proliferation and survival despite EGFR inhibition. Rac-1 is frequently overexpressed in colorectal cancer and has been implicated in the development of resistance to cetuximab therapy. In addition, Rac1-mediated cytoskeletal remodeling contributes to increased cell migration and motility.[27] Indeed, Rac-1 overexpression has been reported as a potential biomarker in colon cancer patients and has been associated with patient survival outcomes. In human tumor-derived organoid cultures, suppression of Rac-1 has been shown to significantly reduce the clonogenic capacity of tumor cells and enhance responses to cetuximab, suggesting a potential role in limiting metastatic potential.[28] On the other hand, although increased Rac-1 expression has been reported in several types of breast cancer, it has also been suggested that cellular dynamics associated with Rac1 can be suppressed following radiotherapy.[29] Furthermore, the inhibition of Rac-1 has been proposed as a promising therapeutic strategy for ER-positive breast cancer.[30] Rac1 regulates the organization of F-actin, which is essential for changes in cell morphology and motility. During this process, cells may also influence surrounding cells through secretory mechanisms.[31] Accordingly, in the present study we investigated Rac-1, Vav-1, and F-actin levels both in the cell supernatant and in cell pellets. Our findings suggest that α-tocopherol may enhance the cellular effects of cetuximab, as reflected by alterations in Vav-1, Rac-1, and F-actin levels. The differential Rac-1 responses observed between the supernatant and cell pellet fractions suggest that treatment effects may vary between extracellular/released and cell-associated Rac-1; however, the present data cannot distinguish altered secretion or protein release from changes in intracellular protein turnover or cellular composition.

Vav-1 is a signaling molecule that functions as a guanine nucleotide exchange factor activating Rho family GTPases, particularly Rac-1. Increased Vav-1 expression in cancer cells has been associated with enhanced cell motility, increased invasive capacity, and sustained proliferative signaling. In early-stage breast cancer, Vav1 expression has been reported to correlate with Akt phosphorylation.[32] In ER-positive breast cancer, estrogen has been shown to modulate the transcription and expression of Vav-1, thereby contributing to the proliferation of cancer cells. Vav-1 activation is frequently regulated by protein kinase C (PKC) and tyrosine kinases. α-tocopherol is known to inhibit PKC activity, and effects of α-tocopherol on Vav1 signaling have also been reported. Therefore, α-tocopherol may interfere at this stage and suppress excessive activation or synthesis of Vav-1.

Vav-1 activation is also sensitive to oxidative stress.[33] By balancing intracellular ROS, α-tocopherol may stabilize stress-induced upregulation of Vav-1. The increase in Vav-1 levels observed after prolonged exposure (e.g., 72 hours) may represent an adaptive escape mechanism developed by cells in response to cetuximab treatment. When EGFR signaling is inhibited, cells may upregulate Vav-1 to activate Rho GTPases as an alternative pathway. The increase in Vav-1 induced by cetuximab alone, representing a potential drug-escape response, appears to be suppressed in the presence of α-tocopherol. Through regulation of F-actin organization, Vav-1 can promote the transition of cells toward a mesenchymal phenotype. In breast cancer, actin and actin-binding proteins regulate key processes involved in tumor progression, including migration, invasion, and metastasis. When F-actin forms membrane protrusions, it facilitates directed cell movement and enhances adhesion to the extracellular matrix, and this can occur independently of receptor signaling pathways in breast cancer cells.[34] Alterations in Rho GTPases such as Rac-1 and Vav-1 can also promote protease secretion, leading to extracellular matrix degradation and enabling cancer cells to overcome tissue barriers and metastasize. These findings identify Vav-1 and Rac-1 as potential molecular candidates associated with the cellular response to combined cetuximab and α-tocopherol treatment and provide a basis for future mechanistic studies. The absence of significant changes in F-actin protein levels at 72 hours, followed by a significant reduction after 7 days, suggests a time-dependent response to the treatments. This delayed alteration may reflect cumulative effects of prolonged treatment on cellular organization and cytoskeletal remodeling. However, the present findings do not establish the precise mechanism underlying this temporal response, and changes in cell number, protein turnover, or cytoskeletal organization may contribute to the observed reduction in F-actin levels.

α-tocopherol may contribute to the cellular effects observed with cetuximab through alterations in Vav-1-associated signaling and actin-related cellular organization. When evaluated in terms of the F-actin-enriched and G-actin-enriched fractions, our results showed that the combination of cetuximab and α-tocopherol was associated with changes in actin distribution. The 50 μM concentration of α-tocopherol should similarly not be considered a direct representation of routine dietary exposure. Nevertheless, human pharmacokinetic studies indicate that α-tocopherol concentrations in the micromolar range can be achieved following supplementation, with substantially increased circulating concentrations reported after high-dose supplementation. Thus, the concentration used in the present study represents a

pharmacologically relevant experimental exposure rather than a physiological dietary concentration.[35]

From the perspective of EMT-associated cellular processes, these findings suggest that the combination treatment may modulate cytoskeletal organization and cellular processes related to tumor progression. However, the observed changes in Vav-1, Rac-1, and F-actin cannot be considered definitive evidence of EMT inhibition or suppression of specific resistance pathways, particularly in the absence of direct canonical EMT and functional assays.

Although the present findings provide preliminary evidence for the potential effects of combined cetuximab and α-tocopherol treatment on cellular proliferation, colony formation, and EMT-related processes, several limitations should be acknowledged. The morphological changes observed in the present study, including increased cell rounding and irregular cell shapes, may reflect alterations in cellular organization and cytoskeletal dynamics; however, these changes cannot be specifically attributed to EMT, as similar morphological features may also occur in response to cellular stress, reduced proliferation, or apoptosis. First, this study was conducted using an in-vitro MCF-7 breast cancer cell model, and therefore the findings may not fully reflect the complex tumor microenvironment and pharmacological conditions observed in patients. In particular, the present results cannot be directly extrapolated to the use of α-tocopherol supplementation in patients receiving cetuximab treatment. Further studies using additional breast cancer models, followed by well-designed clinical studies with larger patient populations, are required to determine whether α-tocopherol supplementation has clinically relevant effects in patients receiving cetuximab-based therapy. Nevertheless, the present findings may provide preliminary experimental evidence and a basis for future translational investigations.

Conclusion

Dietary supplements commonly used by cancer patients during treatment may significantly influence the therapeutic efficacy of anticancer agents. Therefore, studies investigating the dose- and time-dependent interactions between pharmacological treatments and nutritional supplements are essential for improving treatment outcomes. In the present study, the effects of α-tocopherol during cetuximab treatment were evaluated in MCF-7 breast cancer cells, with particular emphasis on cell proliferation, colony-forming capacity, and selected EMT-associated cellular and cytoskeletal components.

Our findings suggest that α-tocopherol may enhance the cellular effects of cetuximab and is associated with alterations in Vav-1, Rac-1, and F-actin levels, particularly following prolonged treatment. The differential responses observed in cell-derived supernatant and cell-associated fractions further indicate that the effects of the combination treatment may vary according to the cellular fraction and treatment duration. These findings provide preliminary evidence that α-tocopherol may modulate cellular and cytoskeletal processes associated with EMT; however, they do not establish direct inhibition of EMT, cellular escape mechanisms, or therapeutic resistance. Although the results of this study are limited by its in-vitro design and the absence of direct assessment of canonical EMT markers, apoptosis, and migration/invasion, the findings provide preliminary data that may guide future mechanistic and preclinical studies. Further investigations using canonical EMT markers, functional migration and invasion assays, apoptosis analysis, and molecular inhibition or

knockdown approaches will be required to clarify the mechanisms underlying the combined effects of α-tocopherol and cetuximab.

Acknowledgments
The authors would like to thank Aydin Adnan Menderes University Science and Technology Application and Research Center (ADU-BILTEM) for technical support.

Funding
This work was supported by Aydin Adnan Menderes University Research Grant (ADU-TPF-23016), The Scientific and Technological Research Council of Turkey (TUBITAK 124S213).

Authors' Contribution
M.A: Data acquisition; Designing the experiments, data analysis, drafting and critical reviewing of the manuscript.
D.Y: Data analysis and data interpretation, draft review.
O. C: Conception of the work, study design, drafting, data approval, edited and approved the final manuscript. All authors have read and approved the final manuscript version and consent to all aspects of the work, including the prompt investigation and resolution of any queries concerning the accuracy or integrity of its components.

Conflict of Interest
None declared.

References
1. Basudan AM. Breast cancer ıncidence patterns in the saudi female population: A 17-year retrospective analysis. *Medicina (Kaunas).* 2022;58(11):1617. doi: 10.3390/medicina58111617. PMID: 36363574; PMCID: PMC9697748.
2. Ye F, Dewanjee S, Li Y, Jha NK, Chen ZS, Kumar A, et al. Advancements in clinical aspects of targeted therapy and immunotherapy in breast cancer. *Mol Cancer.* 2023;22(1):105. doi: 10.1186/s12943-023-01805-y. PMID: 37415164; PMCID: PMC10324146.
3. Ujlaky-Nagy L, Szöllősi J, Vereb G. Disrupting EGFR-HER2 transactivation by pertuzumab in HER2-positive cancer: Quantitative analysis reveals EGFR signal ınput as potential predictor of therapeutic outcome. *Int J Mol Sci.* 2024;25(11):5978. doi: 10.3390/ijms25115978. PMID: 38892166; PMCID: PMC11173106.
4. Cheng X. A comprehensive review of HER2 in cancer biology and therapeutics. *Genes (Basel).* 2024;15(7):903. doi: 10.3390/genes15070903. PMID: 39062682; PMCID: PMC11275319.
5. Qi Y, Deng SM, Wang KS. Receptor tyrosine kinases in breast cancer treatment: unraveling the potential. *Am J Cancer Res.* 2024;14(9):4172-96. doi: 10.62347/KIVS3169. PMID: 39417188; PMCID: PMC11477839.
6. Serna-Gallegos TR, La-Fargue CJ, Tewari KS. The ecstacy of gold: Patent expirations for trastuzumab, bevacizumab, rituximab, and cetuximab. *Recent Pat Biotechnol.* 2018;12(2):101-12. doi: 10.2174/1872083116666171122152131. PMID: 29173192.
7. Li X, Zhao L, Chen C, Nie J, Jiao B. Can EGFR be a therapeutic target in breast cancer? *Biochim Biophys Acta Rev Cancer.* 2022;1877(5):188789. doi: 10.1016/j.bbcan.2022.188789. Epub 2022 Sep 3. PMID: 36064121.
8. Huang Y, Hong W, Wei X. The molecular mechanisms and therapeutic strategies of EMT in tumor progression and metastasis. *J Hematol Oncol.* 2022;15(1):129. doi: 10.1186/s13045-022-

01347-8. PMID: 36076302; PMCID: PMC9461252.
9. Pastushenko I, Blanpain C. EMT transition states during tumor progression and metastasis. *Trends Cell Biol.* 2019;29(3):212-26. doi: 10.1016/j.tcb.2018.12.001. PMID: 30594349.
10. Chen Y, Ding H, Song J, Gao X. Breast neoplasm epithelial-mesenchymal transition and cytokines: a systematic review. *Cancer Cell Int.* 2025;25(1):323. doi: 10.1186/s12935-025-03973-x. PMID: 41024150; PMCID: PMC12482044.
11. Ma N, Xu E, Luo Q, Song G. Rac1: A regulator of cell migration and a potential target for cancer therapy. *Molecules.* 2023;28(7):2976. doi: 10.3390/molecules28072976. PMID: 37049739; PMCID: PMC10096471.
12. Svitkina T. The actin cytoskeleton and actin-based motility. *Cold Spring Harb Perspect Biol.* 2018;10(1):a018267. doi: 10.1101/cshperspect.a018267. PMID: 29295889; PMCID: PMC5749151.
13. Altamura G, Martano M, Matrone A, Corteggio A, Borzacchiello G. Monoclonal antibody cetuximab impairs matrix metalloproteinases 2 and 9, epithelial-mesenchymal transition and cell migration in feline oral squamous cell carcinoma in vitro. *Vet Comp Oncol.* 2024;22(1):149-55. doi: 10.1111/vco.12943. PMID: 38030131.
14. Szewczyk K, Chojnacka A, Górnicka M. Tocopherols and tocotrienols-bioactive dietary compounds; What ıs certain, what ıs doubt? *Int J Mol Sci*. 2021;22(12):6222. doi: 10.3390/ijms22126222. PMID: 34207571; PMCID: PMC8227182.
15. Shahidi F, de Camargo AC. Tocopherols and tocotrienols in common and emerging dietary sources: Occurrence, applications, and health benefits. *Int J Mol Sci.* 2016;17(10):1745. doi: 10.3390/ijms17101745. PMID: 27775605; PMCID: PMC5085773.
16. Ambrogini P, Torquato P, Bartolini D, Albertini MC, Lattanzi D, Di Palma M, et al. Excitotoxicity, neuroinflammation and oxidant stress as molecular bases of epileptogenesis and epilepsy-derived neurodegeneration: The role of vitamin E. *Biochim Biophys Acta Mol Basis Dis.* 2019;1865(6):1098-112. doi: 10.1016/j.bbadis.2019.01.026. PMID: 30703511.
17. Chu CC, Chew SC, Liew WC, Nyam KL. Review article vitamin E: a multi-functional ingredient for health enhancement and food preservation. *Journal of Food Measurement and Characterization*. 2023;17:6144-56. doi: doi:10.1007/s11694-023-02042-z.
18. Caño-Ochoa SD, Ruiz-Aracama A, Guillén MD. Alpha-tocopherol, a powerful molecule, leads to the formation of oxylipins in polyunsaturated oils differently to the temperature ıncrease: A detailed study by proton nuclear magnetic resonance of walnut oil oxidation. *Antioxidants (Basel).* 2022;11(4):604. doi: 10.3390/antiox11040604. PMID: 35453290; PMCID: PMC9031923.
19. Meulmeester FL, Luo J, Martens LG, Mills K, van Heemst D, Noordam R. Antioxidant supplementation in oxidative stress-related diseases: What have we learned from studies on alpha-tocopherol? *Antioxidants (Basel).* 2022;11(12):2322. doi: 10.3390/antiox11122322. PMID: 36552530; PMCID: PMC9774512.
20. Bi Z, Wang W, Zhao L, Wang X, Xing D, Zhou Y, et al. The generation and transformation mechanisms of reactive oxygen species in the environment and their implications for pollution control processes: A review. *Environ Res.* 2024;260:119592. doi: 10.1016/j.envres.2024.119592. PMID: 39002629.

21. Rauf A, Khalil AA, Awadallah S, Khan SA, Abu-Izneid T, Kamran M, et al. Reactive oxygen species in biological systems: Pathways, associated diseases, and potential inhibitors-A review. *Food Sci Nutr.* 2023;12(2):675-93. doi: 10.1002/fsn3.3784. PMID: 38370049; PMCID: PMC10867483.
22. Cevik O, Turut FA, Acidereli H, Yildirim S. Cyclosporine-A induces apoptosis in human prostate cancer cells PC3 and DU145 via downregulation of COX-2 and upregulation of TGFβ. *Turkish Journal of Biochemistry*. 2019;44(1):47-54. doi:10.1515/tjb-2017-0355.
23. Çilesiz Y, Cevik O. Anticancer effect of the letrozole-quercetin combination mediated by FOXOs and estrogen receptors in breast cancer cells. *Journal of Research in Pharmacy*. 2025;25(4):479-89. doi:10.29228/jrp.38.
24. Tomasso MR, Mehetre PD, Nagarajan P, Ravi R, Byrnett J, Brinckman E, et al. Cdc42EP3-bound septin scaffolds promote actin polymerization. *J Biol Chem.* 2025;301(3):108325. doi: 10.1016/j.jbc.2025.108325. PMID: 39971161; PMCID: PMC11952830.
25. Liu H, Zhang B, Sun Z. Spectrum of EGFR aberrations and potential clinical implications: insights from integrative pan-cancer analysis. *Cancer Commun (Lond).* 2020;40(1):43-59. doi: 10.1002/cac2.12005. PMID: 32067422; PMCID: PMC7163653.
26. Habban Akhter M, Sateesh Madhav N, Ahmad J. Epidermal growth factor receptor based active targeting: a paradigm shift towards advance tumor therapy. *Artif Cells Nanomed Biotechnol.* 2018;46(sup2):1188-98. doi: 10.1080/21691401.2018.1481863. PMID: 29991287.
27. Wahoski CC, Singh B. The roles of RAC1 and RAC1B in colorectal cancer and their potential contribution to cetuximab resistance. *Cancers (Basel).* 2024;16(13):2472. doi: 10.3390/cancers16132472. PMID: 39001533; PMCID: PMC11240352.
28. Gudiño V, Pohl SÖ, Billard CV, Cammareri P, Bolado A, Aitken S, et al. RAC1B modulates intestinal tumourigenesis via modulation of WNT and EGFR signalling pathways. *Nat Commun.* 2021;12(1):2335. doi: 10.1038/s41467-021-22531-3. PMID: 33879799; PMCID: PMC8058071.
29. Hein AL, Post CM, Sheinin YM, Lakshmanan I, Natarajan A, Enke CA, et al. RAC1 GTPase promotes the survival of breast cancer cells in response to hyper-fractionated radiation treatment. *Oncogene.* 2016;35(49):6319-29. doi: 10.1038/onc.2016.163. PMID: 27181206; PMCID: PMC5112160.
30. Sun J, Gaidosh G, Xu Y, Mookhtiar A, Man N, Cingaram PR, et al. RAC1 plays an essential role in estrogen receptor alpha function in breast cancer cells. *Oncogene.* 2021;40(40):5950-62. doi: 10.1038/s41388-021-01985-1. PMID: 34373577; PMCID: PMC8497275.
31. Jain P, Guichard A, Moayeri M, Kaduwal S, Mel de Fontenay M, Rousseau I, et al. Anthrax ET activates Rac1 and RTK signaling to induce F-actin reorganization and endothelial permeability. *iScience.* 2025;28(11):113682. doi: 10.1016/j.isci.2025.113682. PMID: 41158867; PMCID: PMC12555787.
32. Grassilli S, Brugnoli F, Lattanzio R, Marchisio M, Perracchio L, Piantelli M, et al. Vav1 downmodulates Akt in different breast cancer subtypes: a new promising chance to improve breast cancer outcome. *Mol Oncol.* 2018;12(7):1012-25. doi: 10.1002/1878-0261.12203. PMID: 29658179; PMCID: PMC6026867.
33. Qiu J, Guo J, Liu L, Liu X, Sun X, Chen H. Vav1 promotes inflammation and neuronal apoptosis in cerebral ischemia/reperfusion injury by upregulating

microglial and NLRP3 inflammasome activation. *Neural Regen Res.* 2023;18(11):2436-42. doi: 10.4103/1673-5374.371368. PMID: 37282474; PMCID: PMC10360116.
34. Alfarafisa NM, Herriyanto RI, Alhaq KF, Fauzi MB, Khairani AF. The role of actin-binding proteins in breast cancer progression. *Breast Cancer (Dove Med Press).* 2026;18:566309. doi: 10.2147/BCTT.S566309. PMID: 41743193; PMCID: PMC12929216.
35. Turck D, Bohn T, Castenmiller J, de Henauw S, Hirsch-Ernst KI, Knutsen HK, et al. Scientific opinion on the tolerable upper intake level for vitamin E. *EFSA J.* 2024;22(8):e8953. doi: 10.2903/j.efsa.2024.8953. PMID: 39099617; PMCID: PMC11294871.

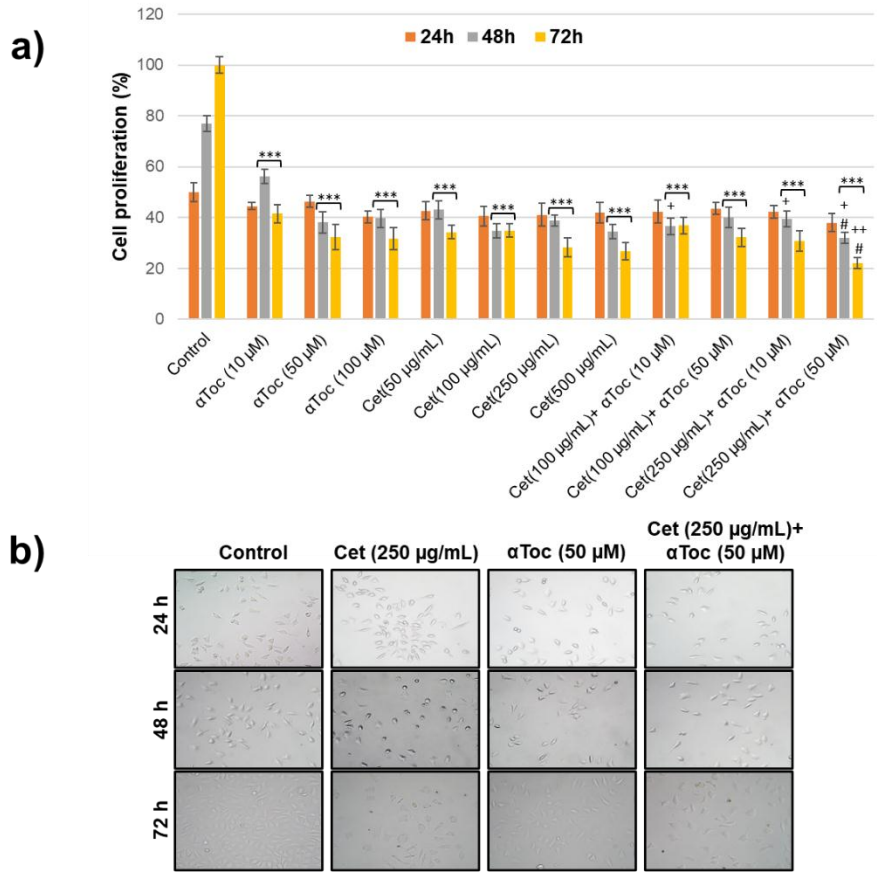


Figure 1. This figure shows the effects of cetuximab and/or α-tocopherol treatment on cell proliferation and morphology of MCF-7 cells. (a) Cell proliferation was evaluated in MCF-7 cells treated with cetuximab at concentrations of 50, 100, 250, and 500 µg/mL or α-tocopherol at concentrations of 10, 50, and 100 µM for 24, 48, and 72 h. The results show the effects of individual treatments on cell proliferation, with statistically significant differences indicated as versus the control group, α-tocopherol-treated group, and cetuximab-treated group. Statistical comparisons were performed within each corresponding time point (24, 48, and 72 h); therefore, each treatment group was compared with its respective time-matched control group. Statistical significance is indicated as *** versus the corresponding control group, $^{+}$ versus the corresponding α-tocopherol-treated group, and $^{\#\#}$ versus the corresponding cetuximab-treated group. Data are presented as mean ± SD. (b) Representative bright-field microscopy illustrating treatment-associated changes in cellular morphology and organization in MCF-7 cells following treatment with Cet (250 µg/mL) and/or αToc (50 µM) for 24, 48, and 72 h.

SD: Standard deviation; Cet: Cetuximab; αToc: α-tocopherol

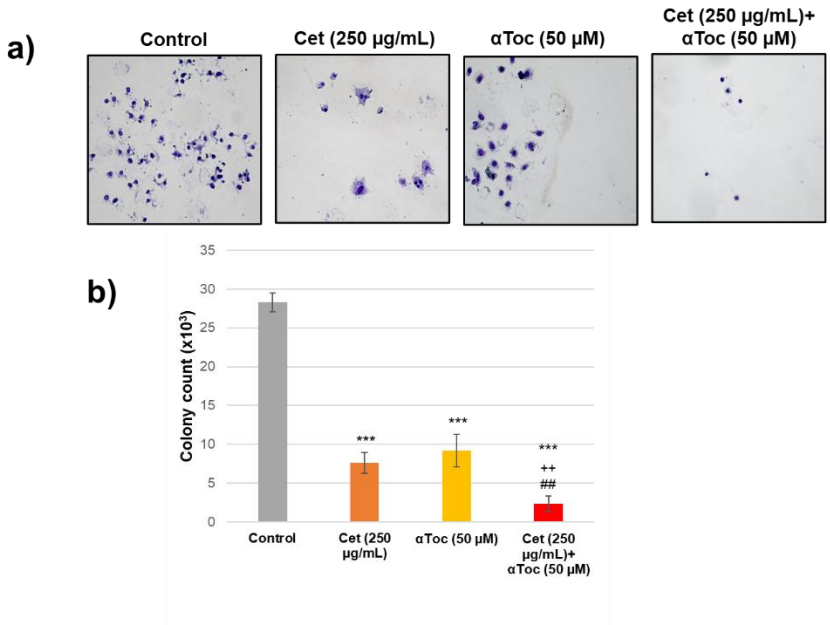


Figure 2. This figure shows the effects of cetuximab and/or α-tocopherol treatment on colony formation and organization in MCF-7 cells. (a) Representative microscopic images show colony formation and cellular interactions in MCF-7 cells following treatment with cetuximab (250 µg/mL) and/or α-tocopherol (50 µM) for 7 days. (b) Quantitative analysis shows the number of colonies formed per well following the indicated treatments. Statistical significance is indicated as *** versus the control group, $^{++}$ versus the α-tocopherol-treated group, and $^{\#\#}$ versus the cetuximab-treated group. Data are presented as mean ± SD.
SD: Standard deviation; Cet: Cetuximab; αToc: α-tocopherol

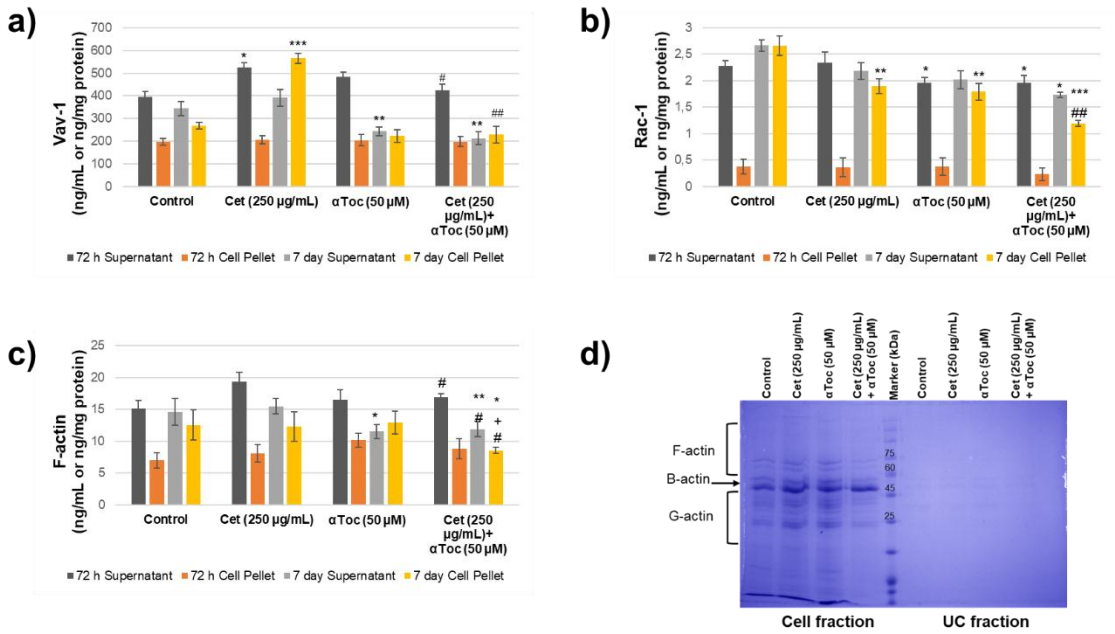


Figure 3. This figure shows the effects of cetuximab and/or α-tocopherol treatment on Vav-1, Rac-1, and F-actin protein levels in MCF-7 cells. (a) Vav-1 protein levels, (b) Rac-1 protein levels, and (c) F-actin protein levels were determined in cell supernatant and pellet samples collected at 72 h and 7 days following treatment with cetuximab (250 µg/mL) and/or α-tocopherol (50 µM) (*, **, *** versus the control group, $^{+}$ versus the α-tocopherol-treated group, and $^{\#}$, $^{\#\#}$ versus the cetuximab-treated group) (d) Representative SDS-PAGE analysis of F-actin- and G-actin-enriched fractions obtained after ultracentrifugation. Following ultracentrifugation, the pellet and supernatant fractions were considered F-actin- and G-actin-enriched fractions, respectively. The band patterns provide qualitative information on actin-associated protein distribution. Data are presented as mean ± SD, with statistical significance indicated in the corresponding panels.

SD: Standard deviation; Cet: Cetuximab; αToc: α-tocopherol; UC: Ultracentrifugation